Investigation of liquid metal embrittlement avoidance strategies for dual phase steels via electro-thermomechanical finite element simulation

M. Biegler[1], C. Böhne[2], G. Seitz[1], G. Meschut[2], M. Rethmeier[4,1,3]

[1] *Fraunhofer Institute of Production Systems and Design Technology (IPK), Berlin, Germany*

[2] *Laboratory for Material and Joining Technology (LWF®), Paderborn, Germany*

[3] *Federal Institute of Materials Research and Testing (BAM), Berlin, Germany*

[4] *Institute for Machine Tools and Factory Management (IWF), TU Berlin, Germany*

Abstract

Modern advanced high-strength steel (AHSS) sheets used in automotive body construction are mostly zinc coated for corrosion resistance. The presence of zinc can cause cracking in steels due to liquid metal embrittlement (LME) during resistance spot welding (RSW). In combination with factors such as tensile strains, liquid zinc can lead to the formation of brittle, intergranular cracks in the weld and heat affected zone. While practical investigations to mitigate LME occurrence exist, the reason why a certain parameter might cause or prevent LME is often unknown. Numerical resistance spot welding simulation can visualize the underlying stresses, strains and temperatures during the welding process and investigate experimentally unmeasurable phenomena.

In this work, a 3-dimensional electro-thermomechanical finite element approach is used to assess and investigate the critical parameters leading to LME occurrence. Experimentally observed crack sizes are correlated with the corresponding local strain rates and temperature exposure durations in the simulation. With this data, a map of LME occurrence over driving influence factors is drafted and discussed for effectiveness.

Introduction

Liquid metal embrittlement (LME) occurrence in advanced high-strength steels is a stochastic phenomenon dependent on the steel substrate material, zinc coating, the resistance spot welding process as well as component topology (i.e. local stiffness) [1]. The degree to which a single factor influences or even causes LME is currently unknown and cannot be easily extracted from experimental data due to low reproducibility and large scatter. So that over the years a lot of different factors have been attributed to cause LME [2, 3]

Numerical simulation offers the possibility to quantify driving factors underlying LME formation such as temperature exposure and local straining of the material. These factors can be correlated with experimentally observed crack occurrence to foster the understanding of LME causes and eventually reach a degree of predictability sufficient for industrial applications.

This work investigates the interdependent influence of two driving factors identified in previous works, i.e. surface temperature exposure time above zinc melting temperature [4, 5] and the local strain rate for the at-risk shoulder of the resistance spot weld [6, 7] . These values are extracted for a number of material thickness combinations and process parametrizations published in previous articles by the authors [4, 5] and set in relation to crack occurrence and severity. Results are then discussed with regards to predictive capabilities and further necessary work for validation and extension of the approach.

Source material

A total of three different setups from previous articles are considered. The reader is directed towards the articles for a detailed description of both the experimental and simulation procedure and the conclusions drawn from the work. The experimental matrix as well as observed crack occurrence for all considered cases is shown in Table 1.

In brief [5] consists of 12 different parametrizations using electrode caps with progressively larger working planes (i.e. 5.5 mm working plane, 8 mm working plane and flat-headed R100 caps with 16mm working plane) as well as progressively increased weld times. The observed trend is that smaller working planes and longer weld times exacerbate LME occurrence. The parameters are shown in Table 1 A-L.

Secondly [4] investigates the influence of temperature exposure duration on the surface by varying the electrode hold time after welding. With increased hold time, LME occurrence is mitigated. On the other hand, inputting larger amounts of energy increases LME occurrence. In the work cited, adding another layer of sheet metal increased the overall thickness of the joint, which allowed greater spatter-free energy input. For a two-sheet stack-up (with a dual phase steel as the top sheet and a mild steel as joining partner) LME does not form for medium hold times. For a 4-sheet stack-up with 3 mild steels at the bottom, LME occurs for these medium hold times. It is concluded that the duration of temperatures above 420°C at the shoulder of the weld drives LME formation. This parameter is one of the two influence factors considered in this work. The parameters are shown in Table 1 M-R.

Lastly, [7] focuses on the role of strain rate for LME occurrence. It could be shown that a small increase in welding current causes a significantly larger strain rate at the shoulder of the weld. In order to evaluate the strain rate in simple setups, it was linked to the electrode cap sink-in velocity via the following equation:

$$v_{elec} = \frac{0.7 * d_{elecMax}}{t_{weld}\{0.7 * d_{elecMax}\}} \quad (1)$$

with v_{elec} expressing the mean electrode indentation velocity in mm/s, $d_{elecMax}$ denoting the maximum electrode sink-in measured between the lowest point of the indentation and the shoulder of the weld in mm and $t_{weld}\{0.7 * d_{elecMax}\}$ denoting the weld time to reach 70 % of $d_{elecMax}$. This value can be extracted from experiments relatively easily, either directly from the weld gun motor or via optical tracking of the electrode movement. It can also be simulated and is therefore suggested as an equivalent measure for strain rate. The parameters are shown in Table 1 S-V.

CODE	WELDING PARAMETERS	ELECTRODE CAP	STACK-UP	LME?
A	Force: 4 kN Weld time: **320 ms** Current: 8.7 kA Hold time: 200 ms	F1-16-20-50-**5.5**	1.34 mm DP1200 HD 2mm mild steel	No
B	Force: 4 kN Weld time: **640 ms** Current: 8.7 kA Hold time: 200 ms	F1-16-20-50-**5.5**	1.34 mm DP1200 HD 2mm mild steel	Light
C	Force: 4 kN Weld time: **960 ms**	F1-16-20-50-**5.5**	1.34 mm DP1200 HD 2mm mild steel	Yes

	Current: 8.7 kA Hold time: 200 ms			
D	Force: 4 kN Weld time: **1280 ms** Current: 8.7 kA Hold time: 200 ms	F1-16-20-50-**5.5**	1.34 mm DP1200 HD 2mm mild steel	Yes
E	Force: 4 kN Weld time: **320 ms** Current: 9.1 kA Hold time: 200 ms	F1-16-20-50-**8.0**	1.34 mm DP1200 HD 2mm mild steel	No
F	Force: 4 kN Weld time: **640 ms** Current: 9.1 kA Hold time: 200 ms	F1-16-20-50-**8.0**	1.34 mm DP1200 HD 2mm mild steel	No
G	Force: 4 kN Weld time: **960 ms** Current: 9.1 kA Hold time: 200 ms	F1-16-20-50-**8.0**	1.34 mm DP1200 HD 2mm mild steel	Light
H	Force: 4 kN Weld time: **1280 ms** Current: 9.1 kA Hold time: 200 ms	F1-16-20-50-**8.0**	1.34 mm DP1200 HD 2mm mild steel	Yes
I	Force: 4 kN Weld time: **320 ms** Current: 9.7 kA Hold time: 200 ms	**A0-16-20-100**	1.34 mm DP1200 HD 2mm mild steel	No
J	Force: 4 kN Weld time: **640 ms** Current: 9.7 kA Hold time: 200 ms	**A0-16-20-100**	1.34 mm DP1200 HD 2mm mild steel	No
K	Force: 4 kN Weld time: **960 ms** Current: 9.7 kA Hold time: 200 ms	**A0-16-20-100**	1.34 mm DP1200 HD 2mm mild steel	No
L	Force: 4 kN Weld time: **1280 ms** Current: 9.7 kA Hold time: 200 ms	**A0-16-20-100**	1.34 mm DP1200 HD 2mm mild steel	No
M	Force: 4.5 kN Weld time: 1520 ms Current: 9.3 kA Hold time: **10 ms**	**A0-16-20-100**	1.58 mm DP1200 HD 2mm mild steel	Yes
N	Force: 4.5 kN Weld time: 1520 ms Current: 9.3 kA Hold time: **200 ms**	**A0-16-20-100**	1.58 mm DP1200 HD 2mm mild steel	No
O	Force: 4.5 kN Weld time: 1520 ms Current: 9.3 kA Hold time: **800 ms**	**A0-16-20-100**	1.58 mm DP1200 HD 2mm mild steel	No
P	Force: 4.5 kN Weld time: 1520 ms Current: 9.3 kA Hold time: **10 ms**	**A0-16-20-100**	1.58 mm DP1200 HD 2mm mild steel 2mm mild steel 2mm mild steel	Yes
Q	Force: 4.5 kN Weld time: 1520 ms	**A0-16-20-100**	1.58 mm DP1200 HD 2mm mild steel	Yes

	Current: 9.3 kA Hold time: **200 ms**		2mm mild steel 2mm mild steel	
R	Force: 4.5 kN Weld time: 1520 ms Current: 9.3 kA Hold time: **800 ms**	**A0-16-20-100**	1.58 mm DP1200 HD 2mm mild steel 2mm mild steel 2mm mild steel	No
S	Force: 4.5 kN Weld time: **760 ms** Current: **8.0 kA** Hold time: 300 ms	F1-16-20-50-**5.5**	1.58 mm DP1000 HD 2mm mild steel	No
T	Force: 4.5 kN Weld time: **1520 ms** Current: **8.0 kA** Hold time: 300 ms	F1-16-20-50-**5.5**	1.58 mm DP1000 HD 2mm mild steel	No
U	Force: 4.5 kN Weld time: **760 ms** Current: **9.2 kA** Hold time: 300 ms	F1-16-20-50-**5.5**	1.58 mm DP1000 HD 2mm mild steel	Yes
V	Force: 4.5 kN Weld time: **1520 ms** Current: **9.2 kA** Hold time: 300 ms	F1-16-20-50-**5.5**	1.58 mm DP1000 HD 2mm mild steel	Yes

Simulation procedure

The simulation procedure is described in-detail in [6], in brief an electro-thermo-mechanical RSW simulation is built in the commercial FE-software Simufact.Welding 2021.1. Material properties are scaled from [8] and contact resistances measured according to [9]. After each simulation, a point of interest was defined 0.5 mm outside of the electrode indentation. At this spot, the duration that temperatures exceeded 420 °C was extracted. In order to calculate v_{elec} the difference between deepest point of the indentation and the point of interest was calculated in z-direction and then evaluated using Equation (1).

Results and Discussion

The resulting temperature exposure duration and v_{elec} are plotted together with colour indications for crack severity in Figure 1. Matching parameter sets are linked by lines and the colour code distinguished between the three articles.

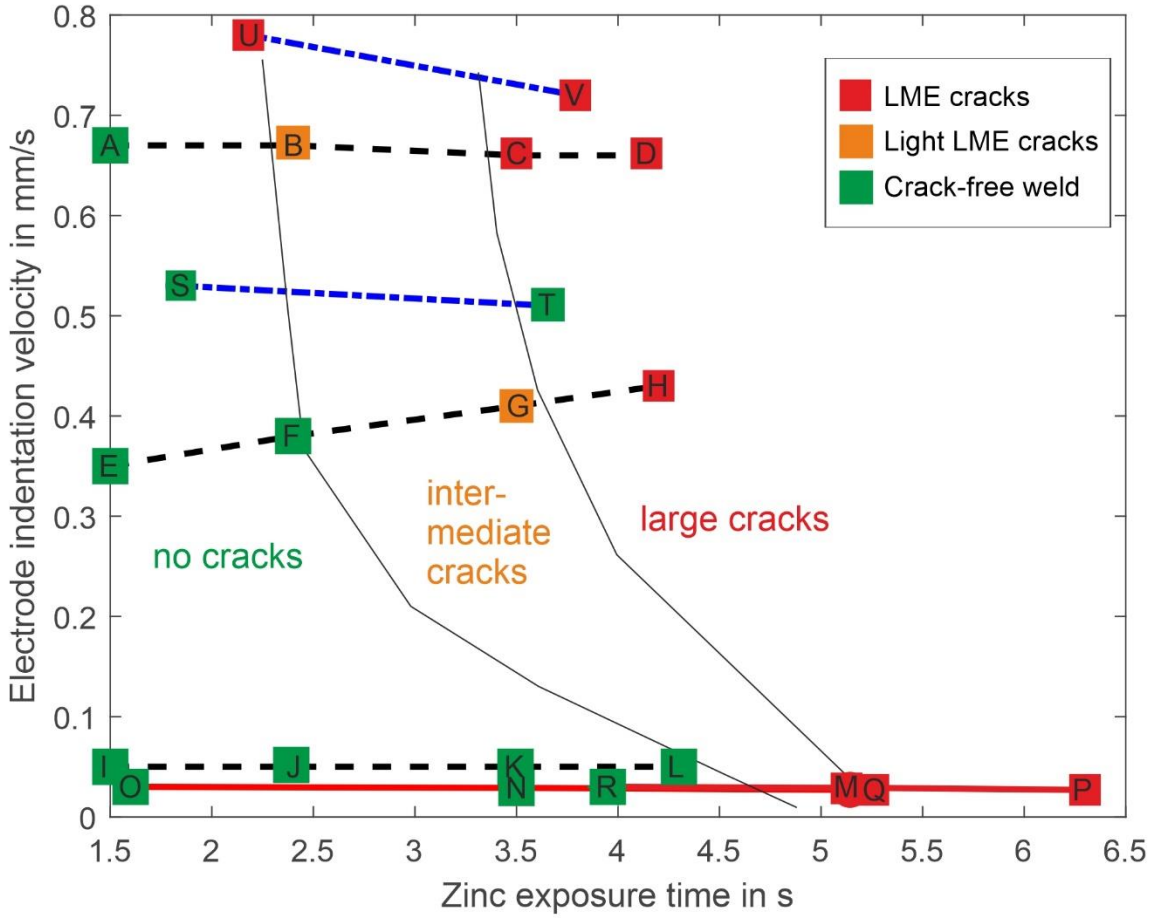

Figure 1: Electrode indentation velocity over liquid zinc exposure time in regards to LME crack occurrence graphic.

In the Figure, a clear dependency between electrode indentation rate, liquid zinc exposure time and cracking is visible. With very high indentation rates and low temperature exposure LME is visible and vice-versa (case U and M, Q and P). If none of the values are very high, a combination of electrode indentation velocity and liquid zinc exposure increases LME likelihood (parameters C, D and H). With lower values for the occurrence factors, LME also decreases. Whereas conclusive data is lacking for the exact shape of the "LME risk areas", a hyperbolic influence can be inferred.

The parameters from [7] (S to V) are outliers, especially T should be crack-afflicted and U nearly crack-free. The investigations use a DP1000 HD steel instead of the DP1200 HD used in all other data sets. It is expected that materials from the same class behave somewhat similarly but do not share the exact same threshold values for risk factors.

In addition, it is currently unclear how to incorporate more complex setups in this model. The parameter v_{elec} is well-defined for an academic case on a single sheet. It cannot easily accommodate electrode misalignment, varying stiffnesses or gaps in real-world setups. It needs to be further developed for these cases.

Conclusion

Existing data from previous publications has been re-evaluated in regards to electrode sink-in velocity (a measure for surface strain rate) and liquid Zinc exposure time.

- This evaluation shows a good overview of the interdependency of the LME influence factors and could be considered an outline of a graphic LME prediction criterion.
- Process deviations (i.e. misaligned electrodes) and external influence factors (i.e. surrounding stiffnesses and gaps) still need to be accounted for in the criterion.
- The criterion will likely need to be adjusted for different steel grades. Simple and meaningful tests will need to be developed derive threshold values for each new material.

Acknowledgement

This work was funded by the Deutsche Forschungsgemeinschaft (DFG, German Research Foundation) – Project-ID 426686311. Grant number RE 1648/11-1; ME 1840/12-1.

References

[1] S. P. Murugan, Y.-D. Park, V. VIJAYAN, and C. Ji, “Four Types of LME Cracks in RSW of Zn-Coated AHSS,” *WJ*, vol. 99, no. 3, 75s-92s, 2020.

[2] E. Wintjes, C. DiGiovanni, L. He, E. Biro, and N. Y. Zhou, “Quantifying the link between crack distribution and resistance spot weld strength reduction in liquid metal embrittlement susceptible steels,” *Weld World*, vol. 63, no. 3, pp. 807–814, 2019.

[3] J.-U. Kim, S. P. Murugan, J.-S. Kim, W. Yook, C.-Y. Lee, C. Ji, J. B. Jeon, and Y.-D. Park, “Liquid metal embrittlement during the resistance spot welding of galvannealed steels: synergy of liquid Zn, α-Fe(Zn) and tensile stress,” *Science and Technology of Welding and Joining*, vol. 26, no. 3, pp. 196–204, 2021.

[4] C. Böhne, G. Meschut, M. Biegler, and M. Rethmeier, “Avoidance of liquid metal embrittlement during resistance spot welding by heat input dependent hold time adaption,” *Science and Technology of Welding and Joining*, vol. 25, no. 7, pp. 617–624, 2020.

[5] C. Böhne, G. Meschut, M. Biegler, J. Frei, and M. Rethmeier, “Prevention of liquid metal embrittlement cracks in resistance spot welds by adaption of electrode geometry,” *Science and Technology of Welding and Joining*, vol. 39, no. 4, pp. 1–8, 2019.

[6] J. Frei, M. Biegler, M. Rethmeier, C. Böhne, and G. Meschut, “Investigation of liquid metal embrittlement of dual phase steel joints by electro-thermomechanical spot-welding simulation,” *Science and Technology of Welding and Joining*, vol. 90, pp. 1–10, 2019.

[7] C. Böhne, G. Meschut, M. Biegler, and M. Rethmeier, “Influence of electrode indentation rate on liquid metal embrittlement formation during resistance spot welding,” *Welding journal*, vol. 101, no. 7, 2022.

[8] C. Schwenk and M. Rethmeier, “Material Properties for Welding Simulation—Measurement, Analysis, and Exemplary Data,” *Welding journal*, vol. 90, no. 11, 2011.

[9] *Instruction sheet for measurement of contact resistance - Fundamentals, measurement methods and equipment (German version)*, Merkblatt DVS 2929-1:2014-08, DVS, 2014.